potentials evaluated by two new statistical tests. *Electroencephalogr Clin Neurophysiol* 57:571–580, 1984.

Möcks, J.; Kohler, W.; Gasser, T.; and Tuan, D.P. Novel approaches to the problem of latency jitter. *Psychophysiology* 25(2):217–226, 1988.

Nelder, J.A., and Mead, R. A simplex method for function minimization. *Computat J* 7:308–313, 1965.

Nunez, P.L. *Electric Fields of the Brain.* New York: Oxford Press, 1981.

Perrin, F.; Pernier, J.; Bertrand, O.; and Echallier, J.F. Spherical splines for scalp potential and current density mapping. *Electroencephalogr Clin Neurophysiol* 72:184–187, 1989.

Raz, J., and Fein, G. Testing for heterogeneity of evoked potential signals using an approximation to an exact permutation test. *Biometrics* 1991, in press.

Raz, J.; Turetsky, B.; and Fein, G. Selecting the smoothing parameter for estimation of smoothly changing evoked potential signals. *Biometrics* 45(3):745–762, 1989.

Raz, J.; Turetsky, B.; and Fein, G. Frequency domain estimation of the parameters of human brain electrical dipoles. *J Am Stat Assoc* 1991, in press.

Sammaritano, M.; de Lotminiere, A.; Andermann, F.; Olivier, A.; Gloor, P.; and Quesney, L.F. False lateralization by surface EEG of seizure onset in patients with temporal lobe epilepsy and gross focal cerebral lesions. *Ann Neurol* 21(4):361–369, 1987.

Scherg, M. *Brain Electrical Source Analysis* (BESA). McLean, VA: Neuroscan, Inc., 1989*a*.

Scherg, M. Fundamentals of dipoles source potential analysis. In: Hoke, M.; Grandori, F.; and Romani, G.L., eds. *Auditory Evoked Magnetic Fields and Potentials.* Basel: Karger, 1989*b*.

Scherg, M., and Von Cramon, D. Two bilateral sources of the late AEP as identified by a spatiotemporal dipole model. *Electroencephalogr Clin Neurophysiol* 62:32–44, 1985.

Scherg, M., and Von Cramon, D. Evoked dipole source potentials of the human auditory cortex. *Electroencephalogr Clin Neurophysiol* 65:344–360, 1986.

Snidman, N., and Kagan, J. Infant predictors of inhibited and uninhibited profiles. *Psychophysiology Suppl* 27:S9–S10, 1990.

Stassen, H.H.; Bomben, G.; and Propping, P. Genetic aspects of the EEG: An investigation into the within-pair similarity of monozygotic and dizygotic twins with a new method of analysis. *Electroencephalogr Clin Neurophysiol* 66:489–501, 1987.

Turetsky, B., and Fein, G. Partitioning of deep vs. superficial evoked potential sources using current source densities is not valid. *Brain Topog* 1991, in press.

Turetsky, B.; Raz, J.; and Fein, G. Estimation of trial-to-trial variation in evoked potential signals by smoothing across trials. *Psychophysiology* 26(6):700–712, 1989.

Turetsky, B.; Raz, J.; and Fein, G. Representation of multi-channel evoked potential data using a dipole component model of intra-cranial generators: Application to the auditory P300. *Electroencephalogr Clin Neurophysiol* 76:540–566, 1990.

In: Zakhari, S. and Witt, E. (eds.),
NIAAA Research Monograph No. 21. Imaging in Alcohol Research.
NIH Publication, Rockville, MD (1992).

5

THE TOPOGRAPHIC ANALYSIS OF MODEL-REFERENCED EVOKED POTENTIAL COMPONENTS

John Odencrantz,[1] Sean O'Connor,[2] Henri Begleiter,[1] and Guowang Zhang[1]

Event-related potentials (ERP) have been used to study cognitive processes in the normal human brain as well as to assess brain function in various types of patient populations. ERP offer a unique approach for examining multiple levels of brain functioning. Quantitative measurements of salient features extracted from ERP recordings reflect various aspects of brain function related to sensory as well as higher integrative processes.

For the most part, ERP represent an amalgam of heterogeneous components. Every component is caused by neuronally induced currents in the brain, with each component manifesting spatial and temporal properties distinct from the other components. Identifying the neural origins of each component would provide fundamental information concerning the functions of the brain. Apart from invasive procedures, which are not feasible except in special circumstances, the only means of obtaining information regarding the locations of the generators is knowledge of the scalp current topographies (e.g., Vaughan et al. 1986).

Decomposition of the evoked potential can be achieved via a number of its known or presumed attributes. Among those proposed are stochastic independence (Donchin 1966), homogeneity across subjects of component spatial properties (Mocks 1988), and geometric and electrophysiological properties of generators (Cuffin and

ACRONYMS

EEG	*electroencephalogram*
ERP	*event-related potential*
MRA	*model-referenced analysis*
SPM	*significance probability map*

[1]*Department of Psychiatry, SUNY Health Sciences Center, Brooklyn, NY 11203*
[2]*Department of Psychiatry, University of Connecticut School of Medicine, Farmington, CT 06032*

Cohen 1977; Kavanagh et al. 1978; Sidman et al. 1978).

We propose a topographic analysis based on a combination of two ideas. The first is a representation of the evoked potential over the head as the product of a matrix specifying the spatial features of the evoked potential and temporal characteristics. Formally

$$\Phi_{l,t}=A_l B_t \qquad (1)$$

where $\Phi_{l,t}$ is the evoked potential at lead l and time t, A_t is a matrix, each column of which determines the spatial configuration of one component, and B_t is a matrix, each row of which specifies the temporal progression of a component. The matrix product has the effect of making the scalp potential a linear combination of a number of underlying source potentials, each of which may vary in strength over time. Such a decomposition is explicit or implicit in the work of a number of researchers, including Maier et al. (1987), Achim et al. (1988), and Turetsky et al. (1990).

Further restrictions are necessary in order to obtain a unique solution to model 1. Mocks (1988) has proposed a related form that draws the necessary restrictions from considerations of consistency between subjects, while Maier et al. (1987) and Achim et al. (1988) use a combination of orthogonality over time and dipole generator theory over space. This last, the instantaneous dipole model, specifies an explicit functional form for A_t. In this chapter, we consider an alternative approach of specifying a functional form for the matrix B_t. The resulting decomposition is unique, thus allowing us to examine the topography of various components without making assumptions about the nature and number of sources that generate each.

The functional form for B_t has for each row an exponentially decaying sinusoid

$$B_{i,t}=e^{-\beta(i)t\%}\sin(\omega\,(i)\,t) \qquad (2)$$

This form is determined from known neuronal interactions. Its physical justification is that it can be derived as a consequence of interacting excitatory and inhibitory nerve masses if nonlinear interactions are excluded. This is similar to Freeman's (1975) model of the evoked potential. O'Connor et al. (1983) derived the single lead model independent of Freeman's earlier work and termed it the "model-referenced analysis" (MRA) of evoked brain potentials.

Practical advantages of this representation include reduction in topographical representation, interpretability, and stability. Representational reduction is a consequence of the fact that a single map is associated with each component, so that a few maps (on the order of five) are sufficient to contain all of the topographic information for a given evoked potential.

Interpretability and stability are both consequences of the fact that MRA components damp quickly in practice, so that each has most of its activity within the time interval of a single evoked potential peak. It is easy to relate MRA components to activities that have been studied in connection with peak analysis; they tend to be stable from one subject to another.

Analyses based on model 1 can focus either on the spatial properties of the data or their dynamic properties. Our focus is on topography, especially with regard to topographical differences between different brain states. Our primary tool is the significance probability map (SPM), first used in connection with brain research by Duffy et al. (1981). We suggest some multivariate SPM that allows components to be combined. Discriminant analysis is also used as a global means of assessing differences.

For illustration purposes, we have chosen to analyze a set of data in which differences are experimentally induced rather than being the consequence of uncontrollable factors. Evoked potentials were measured in 24 subjects chosen to be homogeneous with regard to their medical background. Each subject was studied under three conditions known to produce specific differences in the ERP, especially in P3. This repeated-measures approach tends to minimize problems arising from extraneous factors. The topography of P3 was of particular interest in this experiment, and two models, differing in how they modeled P3, were implemented and compared.

MATERIALS AND METHODS

Experimental Procedure

The subjects were 24 neurologically intact healthy males between the ages of 18 and 24. None had any past history of chronic medical problems. Subjects were seated in a sound-attenuated chamber and told to fixate on the center of a CRT 44 cm away. They were presented with three types of stimuli, each consisting of a straight line (42 mm) rotated into one of three possible orientations and passing through the point of visual fixation. The visual angle was 5.46°. The stimuli were presented one at a time in a random rate (2–5 seconds). The nontarget stimuli were frequently occurring vertical lines (75 percent). Two types of rarely occurring target stimuli were used: an easily recognized line that differed from the vertical by 90° (horizontal) and a difficult-to-recognize target that differed from the vertical by only 3°. The targets were each presented 12.5 percent of the time. The subjects' task was to press a button to all nonvertical stimuli as quickly as possible in a target-selection, reaction-time paradigm.

Electrodes

The entire 10/20 International system of electrodes was used (Electro-Cap), with the nasion serving as a reference and the forehead as a ground. Vertical and horizontal eye leads monitored possible eye movement contamination, and trials with excessive eye movement (>75 μV) were removed.

Event-Related Potentials

The ERP were amplified 20,000 times and were sampled for 100 milliseconds preceding the stimulus (prestimulus baseline) and for 1,000

milliseconds following the stimulus every 5 milliseconds (200 Hz sampling rate; band width 0.1–100 Hz). On-line digital filtering was performed on the data between 0.1 and 30 Hz.

Decomposing the Evoked Potential (MRA)

Our decomposition was based on the following dynamic model of the evoked potential:

$$\Phi_{l,t}=\sum_i A_{i,l} e^{\beta(i)\,(t-t(i))} \sin(\omega\,(i)(t-t(i))\,)\; I(t>t(i)) \quad (3)$$

$\Phi_{l,t}$ is the evoked potential at lead l and time point t, and $A_{i,l}$, $\beta(i)$, $\omega(i)$, and $t(i)$ are a set of parameters associated with the ith evoked potential component. The model assumes that each component has the form of an impulse at time t(i) followed by a damped oscillation. The rate of decay is determined by $\beta(i)$, and the rate of oscillation is $\omega(i)/2\pi$. The $\{A_{i,l}\}$ are the gains at individual leads.

Model 2 was fit to each subject's waveforms averaged over all trials for each of the three target stimuli using a nonlinear optimization procedure with a set of 100 randomly generated starting values.

Two decompositions attempted are shown in the next section, entitled Results. One consisted of four components, the bare minimum necessary to model the evoked potential elicited by a visual target paradigm in the interval between 20 and 2,058 milliseconds. The visible activity consists of P1, which was ignored because of its relatively small size, N1, P2, N2, P3, and late slow activity concentrated in the frontal leads and probably corresponding to the slow wave. It was omitted from consideration in testing for differences between stimulus conditions.

This activity can be minimally fit by a single component concentrated on N1, a second component for P2 and N2, a third component for P3, and a fourth component for the slow wave late activity. The second model for the evoked potential includes all of the components of the minimal model and an additional second component for P3. This component has higher frequency than the first.

Topographic Analysis

The topographies of individual components are displayed as current source density maps. Current densities were computed by the Laplacian derivatives of the potentials, using the spherical spline approach of Perrin et al. (1989).

An indicator of the possible usefulness of the method is its ability to separate the evoked potentials elicited by different stimulus conditions. With this in mind, statistical tests for differences in component potentials and current source densities between stimulus conditions were carried out. Significance probability maps were constructed from these tests.

The next section, entitled Results, gives examples of the kinds of significance probability maps that are appropriate for this problem. They include both univariate (Student's t) and multivariate (Hotelling's T^2) maps, the latter used as a means of combining the information for closely associated distance measures. Two examples of the latter are given. The first is distance, based jointly on two or more components, such as those that make up the early (N1–P2–N2) activity. The second is a two-way distance measure among the three target conditions (nontarget versus target, easy target versus hard target). The use of such combined measurements is, like the MRA itself, a means of reducing the amount of visual information to be presented. All tests are based on differences within subjects rather than differences between averages.

Both the statistics themselves and their associated probability measures can be used as bases for maps. The statistics are generally preferable, and we have used them. The Discussion section covers the reason for this.

Hotelling's T^2 and stepwise discriminant analysis were used as global measurements of topographical distances among the stimulus conditions. The Hotelling's T^2 was based on a nine-dimensional random variable constructed by averaging the potentials of laterally symmetric pairs of leads, excluding the frontal and occipital regions. A separate Hotelling's T^2 test was done for each component and for both target/nontarget and easy target/hard target dichotomies. Both three-way (all target conditions) and two-way (target versus nontarget) discriminant analyses were performed. Equal prior probabilities were specified, so that the overall null expected misclassification was two-thirds for the three-way discriminant analysis and one-half for the two-way discriminant analysis. Cross-validation was used as a means of estimating errors.

RESULTS

Two models, one consisting of four exponentially decaying sinusoidal components and the other consisting of five such components, are summarized in table 1, which gives the values of the parameters for the grand mean of the 24 subjects. Each component is specified by three parameters: the time at which its activity begins (t), the rate at which it decays (β), and the frequency at which it oscillates ($\omega/2\pi$). As explained in the beginning of this chapter, these parameters are the same for all leads. We have also included the peak time and the goodness of fit statistic for the model. This last is the ratio of the sum of squares of errors to the sum of squares of total (SSE/SST).

Figure 1 gives the set of topographic maps for the four-component model under the easy target condition. Because of the independence of the dynamic and spatial properties of the model, these maps and the traces of the individual components at any lead carry all the model's information. The topographic map of each component corresponds to its current source density at its peak.

Table 1. Averaged MRA components

	Nontarget			Easy target			Hard target		
	β	ω	t	β	ω	t	β	ω	t
A1	11.384	19.834	.1066	10.593	18.406	.1081	10.548	17.598	.1104
A2	13.368	24.448	.1633	12.155	23.622	.1617	12.073	24.995	.1618
A3	4.828	6.992	.2330	4.131	6.660	.2577	4.292	5.639	.2579
A4	3.349	2.710	.5115	2.657	2.496	.5373	2.748	2.457	.5308
B1	9.522	24.599	.1112	10.424	24.058	.1113	9.254	24.441	.1076
B2	10.619	22.869	.1599	8.589	21.445	.1610	9.574	21.207	.1530
B3	6.551	7.104	.2434	5.627	6.637	.2576	5.972	6.926	.2587
B4	3.472	10.476	.2403	3.218	9.564	.2448	3.524	9.866	.2463
B5	3.009	2.438	.4634	3.332	2.565	.4974	2.662	2.449	.4792

The components of the four-component model are denoted A1 through A4, and the components of the five-component model are denoted B1 through B5. A1 and A2 are essentially identical to B1 and B2: For both models, these fit the early N1–P2–N2 activity, with A1 and B1 essentially fitting N1. As the topographic maps show, these components are in the lateral parietal and occipital regions. A4 is also clearly identifiable with B5, both components fitting a slow activity located frontally that follows P3. This component is probably the slow wave.

B3 and B4 correspond jointly to A3, which fits P3. In both its frequency and its topography, B3 resembles A3 much more closely than

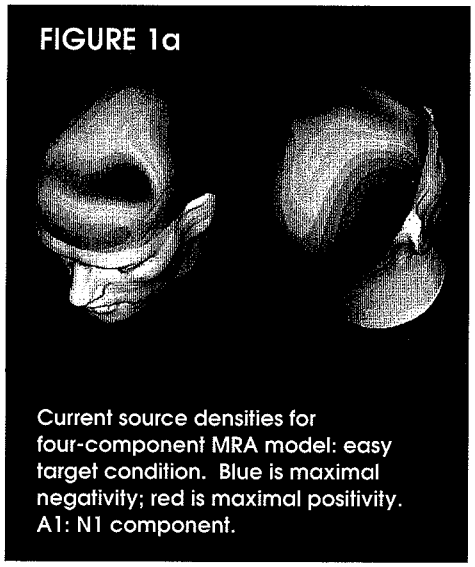

FIGURE 1a

Current source densities for four-component MRA model: easy target condition. Blue is maximal negativity; red is maximal positivity. A1: N1 component.

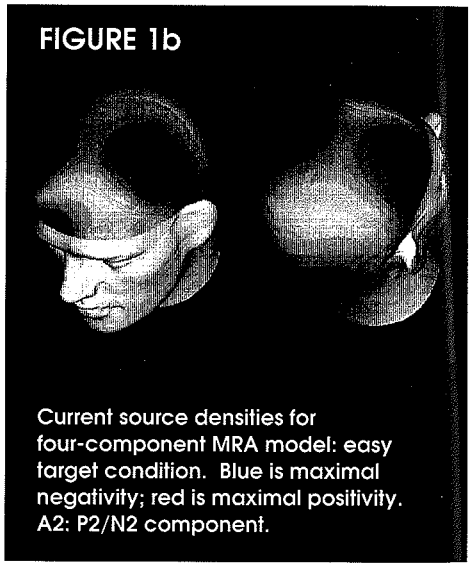

FIGURE 1b

Current source densities for four-component MRA model: easy target condition. Blue is maximal negativity; red is maximal positivity. A2: P2/N2 component.

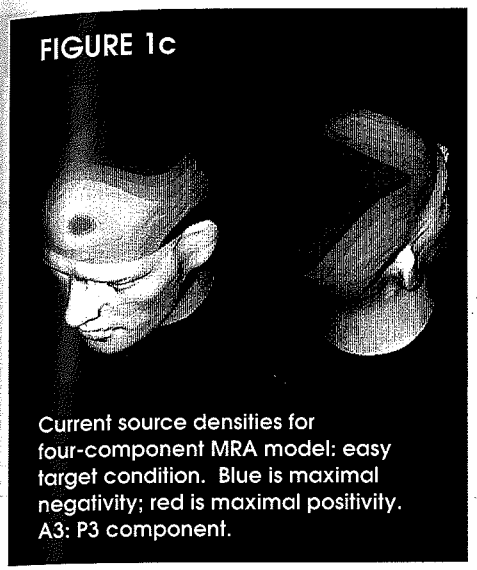

FIGURE 1c

Current source densities for four-component MRA model: easy target condition. Blue is maximal negativity; red is maximal positivity. A3: P3 component.

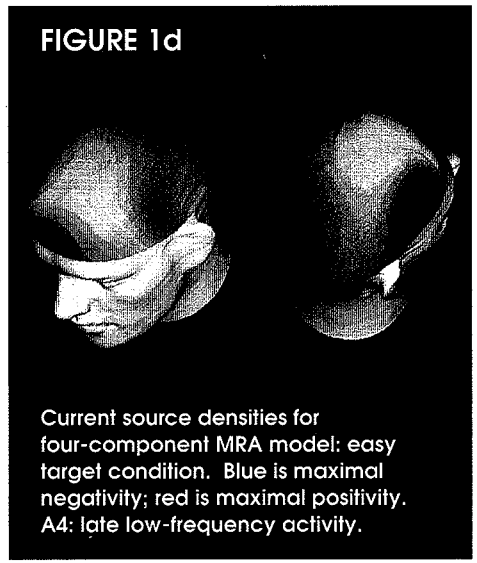

FIGURE 1d

Current source densities for four-component MRA model: easy target condition. Blue is maximal negativity; red is maximal positivity. A4: late low-frequency activity.

does B4 and may be taken to be the primary P3 component. B4 is a possible secondary P3 component; it seems to be both frontal and parietal but not central. It may reflect the contributions of two distinct generators; alternatively, the parietal activity might be a consequence of the limitations of the MRA due to nonlinearities. B4 was not used in the statistical analysis.

Table 2 summarizes the results of the Hotelling's T^2 tests both for potential and current source density. A3, which corresponds to P3, showed the greatest differences (p=0.004 for potential, p=0.007 for current density) between target and nontarget. A2, the joint P2–N2 com-

Table 2. Hotelling's T^2 for global differences

	Nontarget/target			Easy target/hard target		
	F	df	p	F	df	p
A1	1.498	9,16	.230	.977	9,16	.493
	(1.405)	(9,16)	(.265)	(.852)	(9,16)	(.583)
A2	3.470	9,16	.015	2.675	9,16	.041
	(2.788)	(9,16)	(.035)	(2.510)	(9,16)	(.052)
A3	4.594	9,16	.004	.747	9,16	.664
	(4.034)	(9,16)	(.007)	(.800)	(9,16)	(.622)

Entries in parentheses are derived from current source density estimates, and the corresponding potential derived values are above them.

Table 3. Three-way classification

	Resubstitution			Cross-validation		
	Nontarget	Easy target	Hard target	Nontarget	Easy target	Hard target
Nontarget	100.00 (79.19)	0.00 (12.50)	0.00 (8.33)	91.67 (75.00)	4.17 (16.67)	4.17 (8.33)
Easy Target	4.17 (16.67)	83.33 (66.67)	12.50 (16.67)	12.50 (16.67)	58.33 (62.50)	29.17 (20.83)
Hard Target	4.17 (29.17)	8.33 (20.83)	87.50 (50.00)	16.67 (33.33)	20.83 (25.00)	62.50 (41.67)

Entries are percent classified into column. Entries in parentheses are derived from current source density estimates.

ponent, showed appreciable differences both for target/nontarget (p=0.015 for potential, p=0.035 for current density) and for easy target/hard target (p=0.041 for potential, p=0.052 for current density). It was the only component to show a strong difference between the two target conditions. A1, the N1 component, showed little difference, either between target and nontarget or between easy and hard target conditions. Significance levels were consistently better for potential than for current source density, but the differences were not large.

Tables 3 and 4 summarize the results of the discriminant analysis. Both two-way and three-way classifications were quite successful; misclassification levels were well below those expected. Classification based on potential was somewhat better than classification based on current source density; for two-way (target versus nontarget) classification, the level of misclassification for current density was more than twice that for potential.

Figures 1–4 summarize the topography of the MRA components. Figure 1 shows the topography of the four-component model for the easy target condition, and figure 2 shows the topography of the five-component model for the hard target condition. Figures 3 and 4 show the topographies of the components of the four-component model for the nontarget and hard target stimuli, respectively.

Figure 5 shows significance probability maps for component A3 of the four-component model. Figures 5a–c are the individual paired t statistics for each of the three targets, and figure 5d is a map of Hotelling's T^2 statistics.

DISCUSSION

The MRA

The MRA approach is one of a number of possible ways to model

Table 4. Two-way classification

Resubstitution		Cross-validation	
Nontarget	Target	Nontarget	Target
8.33 (20.83)	6.25 (18.75)	8.33 (20.83)	10.42 (25.00)

Entries are percent misclassified. Entries in parentheses are derived from current source density estimates.

and fit the elementary components of an evoked potential. Which method one chooses depends on a number of factors and may well differ from problem to problem. Here, the salient features of the MRA and alternative methods are discussed. The alternative methods we consider are principal components analysis, the intersubject decomposition suggested by Mocks (1988), and dipole-based decomposition methods. It should be noted that these methods are not mutually exclusive: A paper by Turetsky et al. (1990) makes use of both dipole modeling and the MRA.

The distinctive feature of the MRA is that it makes use of a dynamic form that can be derived from a set of differential equations describing neuronal interactions. The multilead form assumes in addition that the time required for the signal to propagate through the head is short, relative to the duration of the evoked potential, and that the temporal and dynamic

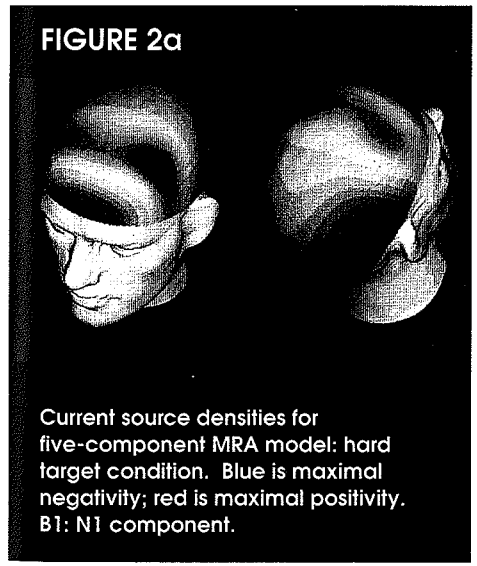

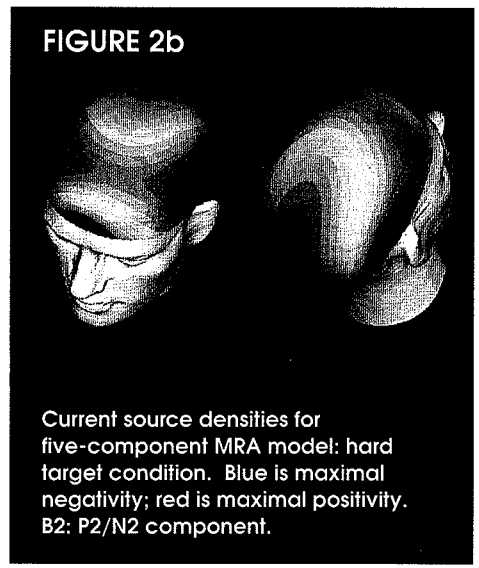

FIGURE 2c

Current source densities for five-component MRA model: hard target condition. Blue is maximal negativity; red is maximal positivity. B3: low-frequency P3 component.

FIGURE 2d

Current source densities for five-component MRA model: hard target condition. Blue is maximal negativity; red is maximal positivity. B4: high-frequency P3 component.

properties of a specific component are independent of each other.

Principal components analysis, which is the earliest method of decomposing evoked potentials (Donchin 1966), is based on the assumption that components are unrelated in their noise. Since this assumption is not sufficient to generate a unique solution, additional, more arbitrary constraints must be added. Those used in practice, such as varimax rotation, are drawn from factor analysis.

FIGURE 2e

Current source densities for five-component MRA model: hard target condition. Blue is maximal negativity; red is maximal positivity. B5: late low-frequency activity.

Mocks' decomposition method is based on the assumption that ERP components differ between subjects only in their relative strengths and not in their individual dynamic or spatial properties. Using this idea, one can replace model 1 with a sum of three-way products:

$$\Phi_{l,s,t}=\sum_j \alpha_{l,j}\beta_{s,j}\gamma_{t,j} \qquad (4)$$

where $\Phi_{l,s,t}$ is the ERP for the subject s at lead l and time t, and where the summation is over the set of components. Mocks shows that this decomposition is unique.

Dipole-based decomposition methods were first used extensively by Scherg and his coworkers (1984, 1985*a*, 1985*b*, 1989), although a

FIGURE 3a

Current source densities for four-component MRA model: nontarget condition. Blue is maximal negativity; red is maximal positivity. A1: N1 component.

FIGURE 3b

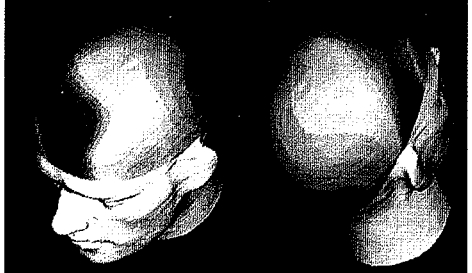

Current source densities for four-component MRA model: nontarget condition. Blue is maximal negativity; red is maximal positivity. A2: P2/N2 component.

FIGURE 3c

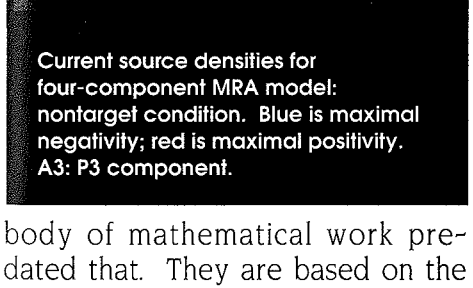

Current source densities for four-component MRA model: nontarget condition. Blue is maximal negativity; red is maximal positivity. A3: P3 component.

FIGURE 3d

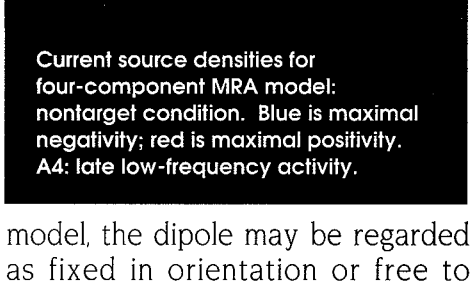

Current source densities for four-component MRA model: nontarget condition. Blue is maximal negativity; red is maximal positivity. A4: late low-frequency activity.

body of mathematical work predated that. They are based on the assumption that the evoked potential is the product of a small number of sources each of which can be approximated by a mathematical point with a linear charge separation. Depending on the particular model, the dipole may be regarded as fixed in orientation or free to change direction, and the dynamic change of the dipole charge may similarly be modeled or left free to vary with the data.

The usefulness of a particular approach depends on a number of

FIGURE 4a

Current source densities for four-component MRA model: hard target condition. Blue is maximal negativity; red is maximal positivity. A1: N1 component.

FIGURE 4b

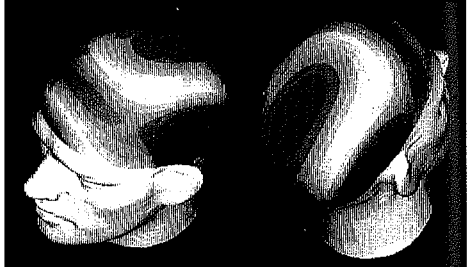

Current source densities for four-component MRA model: hard target condition. Blue is maximal negativity; red is maximal positivity. A2: P2/N2 component.

FIGURE 4c

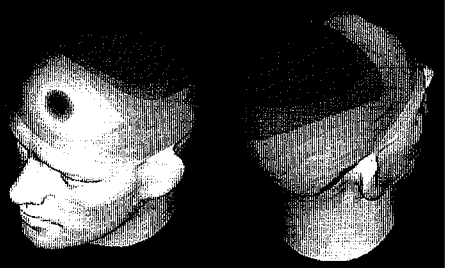

Current source densities for four-component MRA model: hard target condition. Blue is maximal negativity; red is maximal positivity. A3: P3 component.

FIGURE 4d

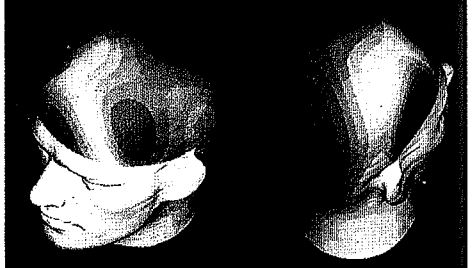

Current source densities for four-component MRA model: hard target condition. Blue is maximal negativity; red is maximal positivity. A4: late low-frequency activity.

factors, including the correctness of a model, its accuracy (given that it is correct), its computational tractability, and its sensitivity to departures from the assumptions on which it is based. With regard to these criteria, the following can be mentioned.

Principal components decomposition is unquestionably the best in terms of its numerical tractability. Not only does it require relatively few computations, but the fact that it does not necessitate a nonlinear search means that its results are exactly replicable when it is conducted twice on the same data. Results of nonlinear optimization will depend on factors extraneous to the model. On the other hand, the assumptions on which principal components are based are tenuous in the biological sense. This is true not only of the rotation criteria in the model, but even the assumption of unrelated noise for different components. While this last seems reasonable, it is in poor accord with the notion of communication between different sources. Principal components analysis has been shown (Wood and McCarthy 1984) to misallocate the signal at least to some degree. Coupled with its weak justification in the first place, this casts doubt on its usefulness.

Mocks' decomposition makes the same spatiotemporal independence

FIGURE 5a

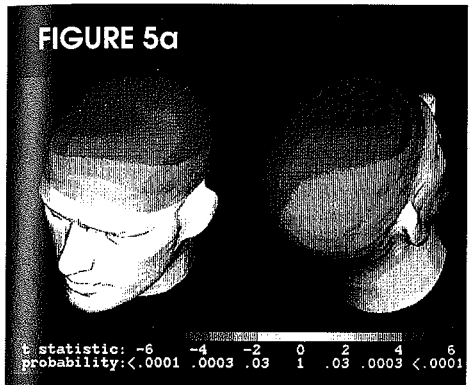

Significance probability maps. Paired t statistic: easy target—nontarget differences.

FIGURE 5b

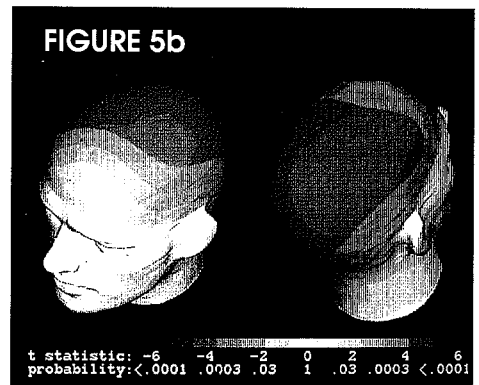

Significance probability maps. Paired t statistic: hard target—nontarget differences.

FIGURE 5c

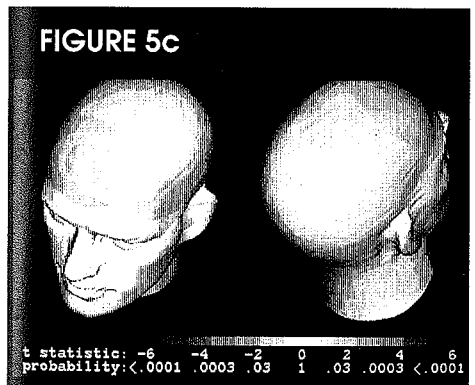

Significance probability maps. Paired t statistic: hard target—easy target differences.

FIGURE 5d

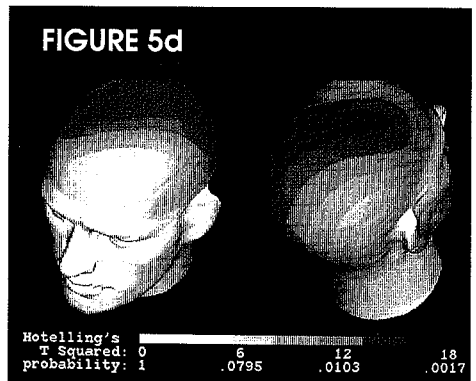

Significance probability maps. Hotelling's T^2 statistic for three-way differences.

assumptions that our MRA model uses. Its defining criterion, that components between individuals differ primarily in their relative strengths, is hard to assess in terms of biological reasonableness. That criterion is clearly an idealization, but it would be useful if the differences in relative strengths were greater than spatial or temporal differences between subjects of their individual components. The biological reasonableness of this is hard to assess on a priori grounds; certainly, it does not follow as a consequence of any model of the brain. It might be interesting to see how the method compares with other decomposition methods when applied to a real data set.

Dipole-based decomposition methods have the advantage that there is no doubt regarding the physical model on which they are based. Evoked potentials certainly originate from charge separations at loci inside the head, and these can be modeled using classical results in electrical field theory. In addition, dipole models do not require that the temporal and spatial aspects of an evoked potential component should be unrelated, because moving and rotating dipoles can be modeled.

An additional advantage of the MRA to a dipole-based decomposition is that it may well require fewer discrete entities for an adequate model because extended dipole sheets may require multiple dipoles for an adequate modeling. An extended dipole sheet producing a coherent MRA component is intrinsically more plausible than a highly localized source producing a dynamically diffuse signal.

In summary, MRA-based decomposition and dipole-based decomposition are the only decomposition methods among those mentioned that have a clear biological justification. Neither is clearly superior to the other in all respects, and which is the appropriate one to use may depend on the specific application. The MRA topographic analysis is more of an exploratory method than dipole modeling.

The Components

We have described the two models that were used and our reasons for believing that the appropriate number of components is either four or five. In the case of the four-component model, there is a clear need for all of the components if all of the most obvious peaks are to be fit. The second P3 component, which is where the models differ, was motivated by topographic features of the data.

An examination of the grand means ERP at all leads showed P3 to be somewhat narrower at the base for the frontal leads than for the coronal and parietal leads, indicating a faster dominant frequency at those leads. Since filtering cannot give rise to new frequencies, the possibility of two distinct components seems likely. Further, it is unlikely that the early activity can be an explanation, partly because its frequency is appreciably higher and partly because it seems to be damped too quickly to account for

an effect observed at the time of P3.

Given that the suggested activities occur cotemporally, it is hard to know how well they could be separated, on the basis of the available data. The topography of B4 shows activity both frontally and parietally but not coronally, which is hard to reconcile as the activity of a single source. A possible explanation for the parietal activity is that there is not a distinct source toward the back, but a system nonlinearity induced by the magnitude of P3. This is a possible shortcoming of the MRA, and it may be necessary to go to nonlinear systems and numerically solved differential equations in order to overcome this. If system nonlinearity is the reason for the parietal topography of B4, P3 could arise from two distinct sources, one located frontally and the other located centrally or parietally, that discharge at about the same time and differ in frequency. Confirmation of that must await further investigation based on more data.

The use of two components to fit the N1–P2–N2 activity is underfitting, at least from the biological perspective. A difficulty with the evoked potential being examined is that the peaks vary greatly in size. P3, for example, is considerably larger than P1. There are severe practical difficulties in fitting components of different scales, and we have not attempted to do so here. Adequate modeling of the early activity would probably necessitate truncating the signal after N2.

Analytical Results

The results of the analysis are supportive of the idea that MRA-based topography can be a useful means of studying evoked potentials and the effects of different brain states. Cross-validated classification levels based on component potentials were good (10 percent two-way misclassification and 30 percent three-way misclassification), and the significance levels and topographic patterns of the significance probability maps correspond reasonably to the results of other studies. Thus, for example, A3 and A1 both have well-defined topographies, but only A3 has strong significance or a well-defined significance topography.

Both the topography and the significance pattern of the A2 and B2 components suggest the involvement of more than one generator, at least for target conditions. The use of a single component under these circumstances is not the best possible solution. As we mentioned in the last subsection, it would probably be necessary to truncate the ERP prior to P3 in order to fit the early activity completely.

SUMMARY

A method of analyzing the topography of evoked potentials, together with some results of applying it to a set of data, have been presented. The results are consistent with what is known from other studies. We have shown that it is possible to distinguish between different stimulus conditions using

this method and to discuss the spatial aspects of the differences.

In recent years, EEG and ERP topographical displays have proved useful in clinical diagnosis and neurological investigations. The practical value of such exploratory methods is supported by the success of the analytically simple BEAM system of Duffy et al. (1979). Our intention is to combine a model-driven decomposition with a data-driven topographical analysis as a means of looking deeper into the data without modeling all aspects of it.

This is not to deny the value of purely modeling efforts such as dynamic dipole models. Such models will doubtless prove extremely useful in understanding the workings of the brain. They can be considered to be the confirmatory part of an analytic effort in which methods such as ours are exploratory and diagnostic. The chief advantage of a method that is partly exploratory in nature is that it depends on fewer assumptions and is more useful in spotting patterns. On the other hand, a method that is only partly exploratory is capable of revealing things that a purely exploratory method might not.

Future improvements of the method could include incorporating nonlinearities into the dynamics and taking into account the autoregressive aspects of the noise.

ACKNOWLEDGMENTS

This study was supported by National Institute on Alcohol Abuse and Alcoholism grants AA-05524 and AA-02686 to Dr.. Henri Begleiter.

REFERENCES

Achim, A.; Richer, F.; and Saint-Hilaire, J.M. Methods for separating temporally overlapping sources of neuroelectric data. *Brain Topogr* 1:22–28, 1988.

Cuffin, B.N., and Cohen, D. Magnetic fields of a dipole in special volume conductor shapes. IEEE *Trans Biomed Eng* 24:372–381, 1977.

Donchin, E. A multivariate approach to the analysis of averaged evoked potentials. IEEE *Trans Biomed Eng* 13:131–139, 1966.

Duffy, F.H.; Bartels, P.H.; and Burchfiel, J.L. Significance probability mapping: An aid in the topographic analysis of brain electrical activity. *Electroencephalogr Clin Neurophysiol* 51:455–462, 1981.

Freeman, W.J. *Mass Action of the Nervous System.* New York: Academic Press, 1975.

Kavanagh, R.N.; Darcey, T.M.; Lehmann, D.; and Fender, D.H. Evaluation of methods for three-dimensional localization of electrical sources in the human brain. IEEE *Trans Biomed Eng* 25:421–429, 1978.

Maier, J.; Dagnelli, G.; Spekreijse, H.; and van Dijk, B.W. Principal components analysis for source localization of VEPs in man. *Vision Res* 22:165–177, 1987.

Mocks, J. Topographic components model for event-related potentials and some biophysical considerations. IEEE *Trans Biomed Eng* 35:482–484, 1988.

O'Connor, S.J.; Tasman, A.; Simon, R.H.; and Hale, M.S. A model referenced method for the identification of evoked potential component waveforms. *Electroencephalogr Clin Neurophysiol* 55:233–237, 1983.

Perrin, F.; Pernier, J.; Bertrand, O.; and Echallier, J.F. Spherical splines for scalp potential and current density mapping. *Electroencephalogr Clin Neurophysiol* 72:184–187, 1989.

Scherg, M. Spatio-temporal modelling of early auditory evoked potentials. *Revue de Laryngologie* 105:103–170, 1984.

Scherg, M.; Vajasar, J.; and Picton, T.W. A source analysis of the late human auditory evoked potentials. J *Cognit Neurosci* 1:336–355, 1989.

Scherg, M., and von Cramon, D. Two bilateral sources of the late AEP as identified by a spatio-temporal dipole model. *Electroencephalogr Clin Neurophysiol* 62:32–44, 1985*a*.

Scherg, M., and von Cramon, D. A new interpretation of the generators of BAEP waves I-V: Results of a spatio-temporal dipole model. *Electroencephalogr Clin Neurophysiol* 62:290–299, 1985*b*.

Sidman, R.D.; Giambalvo, V.; Allison, T.; and Bergey, P. A method for the localization of human cerebral potentials evoked by sensory stimuli. *Sensory Proc* 2:116–129, 1978.

Turetsky, B.; Raz, J.; and Fein, G. Representation of multi-channel evoked potential data using a dipole component model of intracranial generators: Application to the auditory P300. *Electroencephalogr Clin Neurophysiol* 76:540–556, 1990.

Vaughan, H.G.; Weinberg, H.; Lehmann, D.; and Okada, Y. Approaches to defining the intracranial generators of event-related electrical and magnetic fields. *Electroencephalogr Clin Neurophysiol* 38:505–544, 1986.

Wood, C.C., and McCarthy, G. Principal component analysis of event-related potentials: Simulation studies demonstrate misallocation of variance across components. *Electroencephalogr Clin Neurophysiol* 59:249–260, 1984.